

EDINBURGH  
INSTRUMENTS



# PRECISION RAMAN

Best-in-class Raman microscopes  
for research and analytical requirements  
backed with world-class customer  
support and service.



[edinst.com](http://edinst.com)

# Experimental vibrational spectra (Raman, infrared) and DFT calculations on monomeric and dimeric structures of 2- and 6-bromonicotinic acid

Mehmet Karabacak,<sup>a\*</sup> Mehmet Cinar,<sup>a</sup> Sahin Ermec<sup>a</sup> and Mustafa Kurt<sup>b</sup>



In this work, the Fourier transform infrared and Raman spectra of 2-bromonicotinic acid and 6-bromonicotinic acid (abbreviated as 2-BrNA and 6-BrNA,  $C_6H_4BrNO_2$ ) have been recorded in the region 4000–400 and 3500–50  $cm^{-1}$ . The optimum molecular geometry, normal mode wavenumbers, infrared intensities and Raman scattering activities, corresponding vibrational assignments and intermolecular hydrogen bonds were investigated with the help of B3LYP density functional theory (DFT) method using 6-311++G(d,p) basis set. Reliable vibrational assignments were made on the basis of total energy distribution (TED) calculated with scaled quantum mechanical (SQM) method. From the calculations, the molecules are predicted to exist predominantly as the C1 conformer. Copyright © 2009 John Wiley & Sons, Ltd.

Supporting information may be found in the online version of this article.

**Keywords:** 2/6-bromonicotinic acid; IR and Raman spectra; vibrational wavenumbers; DFT; hydrogen bonds

## Introduction

Nicotinic acid and its derivatives have been the subject of investigation for many reasons. Nicotinic acid (widely known as niacin) and its derivatives have good biological activities and versatile bonding modes. The structures of many of the complexes that have been reported show nicotinic acid and its derivatives acting as bridging ligands through the carboxylate group and the pyridyl N atom.<sup>[1]</sup> The solid-state structure of nicotinic acid was first determined in 1953<sup>[2]</sup> and later reinvestigated.<sup>[3]</sup> Nicotinic acid and its complexes with different metals have been thoroughly investigated using different methods.<sup>[4]</sup> The biological importance of this type of compounds and especially its complexes are described in the literature.<sup>[5,6]</sup> Vibrational assignment based on Fourier Transform Infrared (FT-IR) and Raman spectra and theoretical density functional theory (DFT) calculations have been studied for picolinic, nicotinic and isonicotinic acids.<sup>[5]</sup> Sala *et al.*<sup>[6]</sup> investigated vibrational modes of nicotinic acid by both experimental and theoretical methods. Recently, we have investigated the molecular structure and vibrational wavenumbers of 2-chloronicotinic acid<sup>[7]</sup> and 6-chloronicotinic acid<sup>[8]</sup> with IR and Raman spectroscopy and quantum chemical calculations.

To the best of our knowledge, neither quantum chemical calculations nor the vibrational spectra of 2-bromonicotinic acid and 6-bromonicotinic acid have been reported up to now. This inadequacy observed in the literature encouraged us to make this theoretical and experimental vibrational spectroscopic research based on the conformers of the molecules to give a correct assignment of the fundamental bands in the experimental FT-IR and FT-Raman spectra. Therefore, the present study aims to give a complete description of the molecular geometry and molecular vibrations of the 2/6-BrNA.

2/6-BrNA are substituted pyridines with two different functional groups; a Br atom and COOH groups. As model system, nicotinic acid and bromine atom are chosen. The possible stable conformers of 2/6-BrNA molecules were searched. There are four possible conformers for these molecules. The optimized geometry of the conformers and vibrational wavenumbers of 2/6-BrNA were calculated at DFT/B3LYP level of theory using the 6-311++G(d,p) basis set. The variation of energies against the twist angle C3–C2–C7–O9 has been scanned by internal rotation around the C(2)–C(7) single bond to vary every 10° from 0° to 350°. The torsional potential surface of molecules by using semiempirical (AM1) method is shown in Fig. S1 (Supporting Information). The C1 form is the more stable conformer than the others. The vibrational wavenumbers of the C1 dimer conformer of 2/6-BrNA have also been calculated. These calculations are valuable for providing insight into the vibrational spectrum and molecular parameters. A detailed interpretation of the vibrational spectra of 2/6-BrNA has been made on the basis of the calculated total energy distribution (TED).<sup>[9]</sup> The results of the theoretical and spectroscopic studies are reported here.

\* Correspondence to: Mehmet Karabacak, Department of Physics, Afyon Kocatepe University, 03040, Afyonkarahisar, Turkey.  
E-mail: karabacak@aku.edu.tr

<sup>a</sup> Department of Physics, Afyon Kocatepe University, 03040, Afyonkarahisar, Turkey

<sup>b</sup> Department of Physics, Ahi Evran University, 40100, Kirsehir, Turkey

## Experimental

The compounds 2-BrNA and 6-BrNA were purchased from Acros Organics Company with a stated purity 99% and were used as such without further purification. The FT-IR spectra ( $4000\text{--}400\text{ cm}^{-1}$ ) of a KBr disc of the samples were recorded on a Perkin Elmer FT-IR System Spectrum BX spectrometer. FT-Raman spectra of the samples were recorded using the 1064 nm line of a Nd:YAG laser for excitation in the region  $50\text{--}3500\text{ cm}^{-1}$  on a Bruker FRA 106/S FT-Raman spectrometer. The detector was a liquid-nitrogen-cooled Ge detector.

## Quantum Chemical Calculations

The first task for the computational work was to determine the optimized geometry of the compounds. Since the experimental geometries of free 2/6-BrNA are not available, the spatial coordinate positions of 2/6-chloronicotinic acid, as obtained from an X-ray structural analysis,<sup>[10,11]</sup> were used as the initial coordinates for the theoretical calculations. The hybrid B3LYP method<sup>[12,13]</sup> based on Becke's three-parameter functional of DFT and 6-311G++(d,p) basis set level were chosen. Optimized structural parameters were used in the vibrational wavenumbers. The stability of the optimized geometries was confirmed by wavenumber calculations, which gave positive values for all the obtained wavenumbers. TED calculations, which show the relative contributions of the redundant internal coordinates to each normal vibrational mode of the molecule and thus enable us numerically to describe the character of each mode, were carried out by the scaled quantum mechanical (SQM) program<sup>[14,15]</sup> using the output files created at the end of the wavenumber calculations. Calculations were done for four conformers and the dimer structure of the compounds in the ground state, and tabulated only for the most stable monomer (C1) and dimer conformers. All calculations were performed by using the Gaussian 03 program package on a personal computer.<sup>[16]</sup>

## Results and Discussion

The present compounds may have four possible structures. The calculated energies and energy difference of four structures for the title molecules determined by B3LYP are presented in Table S1 (Supporting Information). From DFT calculations, the conformer C1 is predicted to be more stable than other conformers. The 2/6-BrNA molecules consist of 14 atoms, and so they have 36 normal vibrational modes. On the assumption of  $C_s$  symmetry, the number of vibrational modes of the 36 fundamental vibrations is divided into  $25A' + 11A''$ . The vibrations of the  $A'$  species are in-plane modes and those of the  $A''$  species are out-of-plane modes. All fundamental vibrations are active in both IR absorption and Raman scattering. But if the molecule were of  $C_1$  symmetry point group, there would not be any relevant distribution.

### Molecular geometries

Figure S2 (Supporting Information) shows the optimized structures and demonstrates the four possible structures of the compounds with numbering of the atoms. The optimized molecular geometry of the dimer structure is shown in Fig. S3 (Supporting Information). The optimized geometrical parameters calculated by B3LYP with the 6-311++G(d,p) basis set are listed in Table S2

(Supporting Information) in accordance with the atom numbering scheme given in Fig. S2 (Supporting Information). The available experimental geometric parameters for similar compounds are also listed for comparison.<sup>[10,11]</sup> As mentioned above, the results for the most stable conformer and the structures upon dimerization have been tabulated. Intermolecular hydrogen bonds can be responsible for the geometry and the stability of a predominant conformation; the intermolecular O–H...N hydrogen bond between the pyridine N atom-carboxylic acid OH group, and the formation of hydrogen bonding between a hydroxyl group O=COH, cause the structure of the conformer C1 to be the most stable for 2-BrNA and 6-BrNA. In 2-BrNA, the pyridine N atom acts as the hydrogen-bond acceptor and the intermolecular O–H...N hydrogen bonds (the acid-to-pyridine catemeric arrangements) lead to infinite one-dimensional chains. In 6-BrNA, the coplanarity of the carboxylic acid group and the pyridine ring is less than in 2-BrNA, and a weak Br...Br interaction connecting the adjacent dimers may lead to infinite chains.

From the theoretical values, one can find that most of the optimized bond lengths are larger than the experimental values, because the theoretical calculations refer to isolated molecules in the gaseous phase and the experimental results are for molecules in the solid state. It is well known that DFT methods predict bond lengths that are systematically too long, particularly the C–H bond lengths.<sup>[17]</sup> The large deviation from the experimental C–H bond lengths may arise from the low scattering factors of hydrogen atoms in the X-ray diffraction experiment. This overestimation is also verified in our calculation as represented in Table S2 (Supporting Information). Likewise, the calculated O–H value is larger than observed. The obtained C–C bond lengths of the ring fall in the range from 1.379 to 1.397 Å, while the calculated results change from 1.385 to 1.409 Å for the monomer structure. The C–X (F, Cl, Br, etc.) bond length indicates a considerable increase when substituted in place of C–H. The Br atom is in the plane of the pyridine ring. The C–Br bond length are found to be 1.922 Å (2-BrNA) and 1.920 Å (6-BrNA) by using 6-311++G(d,p).

The minimum energy of the 2/6-BrNA dimer structures calculated by the DFT structure optimization method is  $-3010.5204$  and  $-3010.5307$  Hartree, respectively. This interaction arises through the  $O_8\text{--}H_{12}\cdots N_{10}$  and two equivalent stable hydrogen-bonded  $O_8\text{--}H_{12}\cdots O_9$  and  $O_9\text{--}H_{12}\cdots O_8$  contacts, which result in increased stabilization. The O–H distances in the groups involved in the hydrogen bonds are lengthened by 0.030 Å upon dimerization. The shortening of the  $C_7\text{--}O_8$  bond of 6-BrNA (0.034 Å) upon dimerization is due to the redistribution of partial charges on the  $O_8$  atom, as the unpaired electron is significantly delocalized and therefore the C–O bond shows considerable double bond character typical of a carbonyl group. A similar effect was obtained on the angle  $C_7\text{--}O_8\text{--}H_{12}$ .

The optimized bond angles C–C–C and C–N–C in the pyridine ring fall in the range from  $116^\circ$  to  $119^\circ$ , except C2–C3–C4 ( $120.3^\circ$  for 2-BrNA), which is the smaller than hexagonal angle of  $120^\circ$  for the studied molecules. But the C–C–N angles are found to be larger by  $ca\ 4^\circ$  than the hexagonal angles. Similar values are found for other pyridine derivatives.<sup>[7,8,18,19]</sup>

### Vibrational analysis

The FT-IR and FT-Raman spectra of 2/6-bromonicotinic acid are shown in Figs 1 and 2, where the calculated intensities are plotted against the harmonic vibrational wavenumbers. The observed and calculated wavenumbers along with their relative intensities,



probable assignments and TED of 2/6-BrNA are summarized in Tables 1 and 2, respectively. The calculated vibrations for the dimer structures are also presented in these tables. It should be noted that the calculations were made for a free molecule in vacuum, while experiments were performed for solid samples. Furthermore, the anharmonicity is neglected in the real system for the calculated vibrations. Therefore, there are disagreements between the calculated and observed vibrational wavenumbers, and because of the low IR and Raman intensities of some modes, it is difficult to observe them in the IR and Raman spectra. In the last column is given a detailed description of the normal modes based on the TED. All the calculated modes are numbered from the smallest to the biggest wavenumber within each fundamental vibration in the first column of the tables.

The calculated harmonic force constants and wavenumbers are usually higher than the corresponding experimental quantities because of the combination of electron correlation effects and basis set deficiencies. Nevertheless, after applying a uniform scaling factor, the theoretical calculation reproduces the experimental data well. The observed slight disagreement between theory and experiment could be a consequence of the anharmonicity and the general tendency of the quantum chemical methods to overestimate the force constants at the exact equilibrium geometry. Therefore, it is customary to scale down the calculated harmonic wavenumbers in order to improve the agreement with the experiment. In our study, we have followed two different scaling factors, i.e. 0.983 up to 1700  $\text{cm}^{-1}$  and 0.958 for greater than 1700  $\text{cm}^{-1}$ .<sup>[19]</sup>

The Raman activities ( $S_{\text{Ra}}$ ) calculated with the Gaussian 03 program<sup>[16]</sup> were converted to relative Raman intensities ( $I_{\text{Ra}}$ ) using the following relationship derived from the intensity theory of Raman scattering:<sup>[20,21]</sup>

$$I_i = \frac{f(\nu_0 - \nu_i)^4 S_i}{\nu_i [1 - \exp(-hc\nu_i/kT)]}$$

where  $\nu_0$  is the laser exciting wavenumber in  $\text{cm}^{-1}$  (in this work, we have used the excitation wavenumber  $\nu_0 = 9398.5 \text{ cm}^{-1}$ , which corresponds to the wavelength of 1064 nm of a Nd:YAG laser),  $\nu_i$  the vibrational wavenumber of the  $i$ th normal mode (in  $\text{cm}^{-1}$ ) and  $S_i$  is the Raman scattering activity of the normal mode  $\nu_i$ .  $f$  (is a constant equal to  $10^{-12}$ ) is a suitably chosen common normalization factor for all peak intensities.  $h$ ,  $k$ ,  $c$  and  $T$  are Planck and Boltzmann constants, speed of light and temperature in kelvin, respectively.

In aromatic compounds, the C–H stretching wavenumbers appear in the range 3000–3100  $\text{cm}^{-1}$ , and the C–H in-plane and out-of-plane bending vibrations in the range 1000–1300 and 750–1000  $\text{cm}^{-1}$ , respectively.<sup>[22–24]</sup> Accordingly, in the present study, the three adjacent hydrogen atoms left around the ring of 2/6-BrNA give rise to three C–H stretching ( $\nu_{33}$ – $\nu_{35}$ ), three C–H in-plane bending ( $\nu_{23}$ ,  $\nu_{25}$ ,  $\nu_{26}$ ) and three C–H out-of-plane bending ( $\nu_{17}$ – $\nu_{19}$ ) vibrations, which correspond to stretching modes of C3–H11, C4–H6 and C5–H13 units. The aromatic C–H stretching of 2-BrNA gives bands at 3058, 3092, 3161  $\text{cm}^{-1}$  in the IR spectrum and at 3057, 3090  $\text{cm}^{-1}$  in the Raman spectrum. In 6-BrNA, these modes are obtained in the IR spectrum at 3044, 3088  $\text{cm}^{-1}$  and in the Raman spectrum at 3044, 3077  $\text{cm}^{-1}$ . These modes are calculated from 3032 to 3071  $\text{cm}^{-1}$  for 2-BrNA and from 3063 to 3083  $\text{cm}^{-1}$  for 6-BrNA. As expected, these three modes are pure stretching modes as is evident from TED column; they almost contribute 100%. In the IR spectrum, C–H peaks

were observed in the 3042–3104  $\text{cm}^{-1}$  range for nicotinic acid by Koczon *et al.*<sup>[5]</sup> The wavenumbers 1123, 1226, and 1272  $\text{cm}^{-1}$  are assigned for C–H in-plane bending in IR for 2-BrNA, which are in good agreement with values given in literature.<sup>[7,8,25]</sup> The peaks seen at 1139, 1258 and 1281  $\text{cm}^{-1}$  are the corresponding aromatic C–H in-plane bending vibrations of 6-BrNA. The aromatic C–H out-of-plane bending vibrations of 2-BrNA are assigned to the bands observed at 832, 965, and 980  $\text{cm}^{-1}$  in the infrared spectrum. Likewise, for 6-BrNA the corresponding vibrations are assigned at 823, 848, and 952  $\text{cm}^{-1}$ .

The carboxylic acid dimer is formed by strong hydrogen bonding in the solid and liquid state. Vibrational analysis of carboxylic acid is made on the basis of the carbonyl and hydroxyl groups. The band observed in the 1700–1800  $\text{cm}^{-1}$  region due to the C=O stretching vibration is one of the characteristic features of the carboxylic group. The hydrogen-bonded dimer carboxylic acid possesses a form that has a center of symmetry and hence the two monomers can vibrate in-phase and out-of-phase with respect to each other. The in-phase (symmetric) vibrations will be only Raman active, whereas the out-of-phase vibrations will be only IR active. The asymmetric stretch is usually seen at a higher wavenumber than the symmetric stretch.<sup>[22]</sup> On this basis, the vibrational wavenumber described by mode 32 is assigned to the C=O stretching modes. The asymmetrical C=O stretch is observed in IR as strong band at 1718 and 1678  $\text{cm}^{-1}$  (symmetric stretching vibration at 1714 and 1648  $\text{cm}^{-1}$  in Raman) and is predicted at 1707  $\text{cm}^{-1}$  (2-BrNA) and 1716  $\text{cm}^{-1}$  (6-BrNA). The hydrogen-bonding effect through the carboxyl groups, and therefore C=O stretching mode in C1 dimer conformation, was calculated at 1672 and 1709  $\text{cm}^{-1}$  and 1660 and 1663  $\text{cm}^{-1}$  for 2/6-bromonicotinic acid, respectively. In our previous papers,<sup>[7,8]</sup> we assigned the C=O stretching vibration at 1721  $\text{cm}^{-1}$  in FT-IR (1712  $\text{cm}^{-1}$  in FT-Raman) and 1681  $\text{cm}^{-1}$  in FT-IR (1644  $\text{cm}^{-1}$  in FT-Raman) for 2/6-chloronicotinic acid. For nicotinic acid, picolinic acid, and isonicotinic acid this band occurs at 1708, 1717, and 1712  $\text{cm}^{-1}$ , respectively.<sup>[5]</sup>

The carboxylic acid O–H stretching bands are weak in the Raman spectrum, so IR data are generally used. The O–H stretching is characterized by a very broad band appearing near about 3400  $\text{cm}^{-1}$ .<sup>[22,23]</sup> On the other hand, the hydrogen bonding in the condensed phase with the other acid molecules makes vibrational spectra more complicated. Therefore, we could not observe the strong and sharp bands of the O–H vibration in the IR and Raman spectra. However, this band is calculated at 3597 and 3611  $\text{cm}^{-1}$ . In 2-BrNA, the O–H in-plane bending and out-of-plane bending vibrations are assigned to 1405 and 545, 767  $\text{cm}^{-1}$ , respectively. The 6-BrNA in-plane bending vibrations are observed at 1298  $\text{cm}^{-1}$  in the IR spectrum and 1306  $\text{cm}^{-1}$  in the Raman spectrum. A medium band at 542  $\text{cm}^{-1}$  in the FT-IR spectrum is due to the out-of-plane O–H vibration. As seen in Tables 1 and 2, the in-plane bending vibrations are combined with other vibrations. The theoretically computed values are in very good agreement with experimental results. The O–H in-plane and out-of-plane bending vibrations in dimer conformations are increased in value because of the hydrogen-bonding effect through the carboxyl groups.

Assigning the C–N stretching wavenumber is a rather difficult task since there are problems in identifying these wavenumbers from other vibrations. Silverstein *et al.*<sup>[23]</sup> assigned the C–N stretching absorption in the region 1382–1266  $\text{cm}^{-1}$  for aromatic amines. Sundaraganesan *et al.*<sup>[26]</sup> assigned the C–N stretching absorption in the region 1381  $\text{cm}^{-1}$  for 2-amino-5-iodopyridine. In this study, according to the TED assignments, this mode is

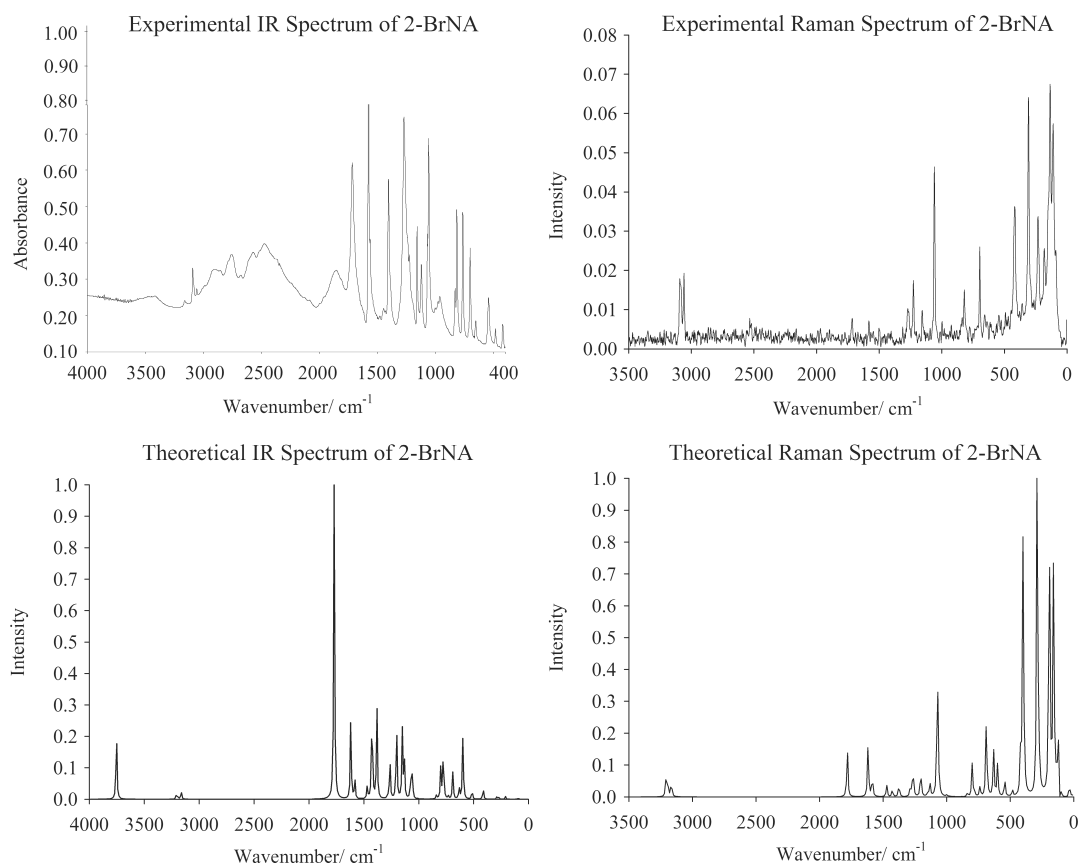


**Figure 1.** The observed and simulated infrared and Raman spectra of 2-bromonicotinic acid.

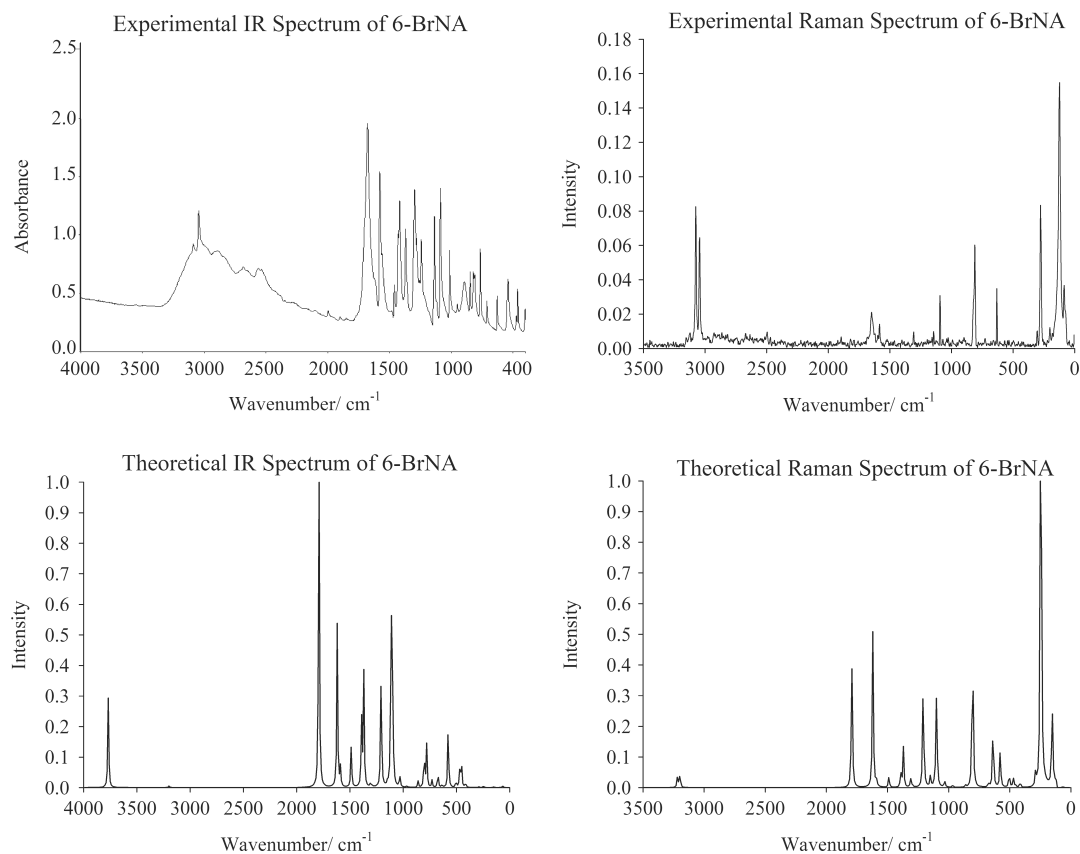


**Figure 2.** The observed and simulated infrared and Raman spectra of 6-bromonicotinic acid.

**Table 1.** The observed FT-IR, FT-Raman and calculated wavenumbers (in  $\text{cm}^{-1}$ ) using B3LYP/6-311++G(d,p) along with their relative intensities, probable assignments and total energy distribution (TED) of monomer and dimer conformers of 2-BrNA.

Experimental		Monomer conformer (B3LYP)					Dimer conformer (B3LYP)			TED ( $\geq 10\%$ )
FT-IR	FT-Ra	Unscaled wavenumbers	Scaled wavenumbers	$I_{\text{IR}}$	$S_{\text{Ra}}$	$I_{\text{Ra}}$	Unscaled wavenumbers	Scaled wavenumbers		
1		35	34	2.1	1.4	0.09	34, 52	33, 51	$\tau$ CCCO (87)	
2	110	98	96	1.8	2.1	0.04	107, 126	105, 124	$\omega$ 2BrNA (90)	
3	136	160	157	0.2	0.9	0.01	164, 174	161, 171	$\delta$ C-COOH (45) + $\delta$ CBr (30)	
4	180	193	190	3.6	1.9	0.02	197, 215	194, 211	$\gamma$ ring def. (75) + $\tau$ COOH (10)	
5	232	276	271	4.6	0.6	0.00	282, 286	277, 281	$\delta$ CBr (44) + $\delta$ ring-COOH (30)	
6	307	289	284	1.3	4.9	0.03	294, 309	289, 304	$\nu$ CBr (60) + $\delta$ C-COOH (20)	
7		398	391	12.0	8.1	0.04	403, 408	396, 401	$\nu$ C-COOH (28) + $\nu$ CBr (21) + $\delta$ OCO (11)	
8	423	415	418	411	2.1	1.5	0.01	421, 423	414, 416	$\gamma$ CCCC (24) + $\gamma$ CCCN (20) + $\gamma$ CCCO (11)
9	485	483	475	0.3	0.3	0.00	484, 488	476, 480	$\gamma$ CCCC (48) + $\gamma$ CCCN (32)	
10		543	534	17.9	1.1	0.00	544, 567	535, 557	$\delta$ C-COOH (40) + $\delta$ CCO (28)	
11	545	600	590	82.3	2.3	0.01	602	592	$\gamma$ OH (82) + $\gamma$ CCCN (10)	
12		631	620	14.2	3.8	0.33	643, 645	632, 634	$\delta$ ring def.(83) + $\delta$ CCO (24)	
13	653	688	676	40.6	8.4	0.61	694, 713	682, 701	$\delta$ COC (33) + $\nu$ CBr (20) + $\delta$ CCC (16) + $\delta$ CCN (12)	
14	704	697	738	725	2.6	1.2	0.08	732, 737	720, 724	$\gamma$ CCCC (40) + $\gamma$ CCNC (40) + $\gamma$ CCCO (18)
15	767		778	765	66.3	0.4	0.02	777, 781	764, 768	$\gamma$ CCCH (45) + $\gamma$ OCOH (42) + $\gamma$ CCCO (28)
16	818	818	799	785	36.9	4.8	0.25	803, 817	789, 803	$\delta$ CCC (40) + $\delta$ C-COOH (21) + $\delta$ CCN (16)
17	832		837	823	7.6	0.7	0.03	837, 844	823, 830	$\gamma$ CH (85) + $\gamma$ CCCO (15)
18	965		980	963	0.1	0.1	0.00	976, 999	959, 982	$\gamma$ CH (91)
19	980		1001	984	0.7	0.3	0.01	1001, 1023	984, 1006	$\gamma$ CH (93)
20	1005		1059	1041	39.8	1.8	0.05	1063, 1070	1045, 1052	$\delta$ CCC (27) + $\delta$ CNC (25) + $\nu$ CO (10)
21	1060	1060	1073	1055	27.2	39.8	1.00	1074, 1075	1056, 1057	Ring breathing (80)
22	1071		1132	1113	68.8	4.7	0.10	1135, 1139	1116, 1120	$\delta$ CH (37) + $\nu$ CO (26) + $\nu$ CC (17) + $\nu$ CN (10)
23	1123		1152	1132	109.8	0.9	0.02	1154	1134	$\delta$ CH (30) + $\nu$ CC (24) + $\nu$ CO (17) + $\nu$ CN (11)
24	1160	1154	1204	1184	85.9	11.2	0.21	1168, 1206	1148, 1185	$\delta$ OH (35) + $\delta$ CH (16) + $\nu$ C-COOH (12)
25	1226	1225	1265	1243	35.5	13.9	0.23	1248, 1266	1227, 1244	$\delta$ CH (31) + $\nu$ CC (20) + $\nu$ CN (20) + $\delta$ COH (12)
26	1272	1268	1286	1264	5.8	4.8	0.08	1283, 1286	1261, 1264	$\nu$ CN (41) + $\nu$ CC (37) + $\delta$ CH (13)
27			1376	1353	116.2	7.4	0.10	1314, 1377	1292, 1354	$\delta$ OH (28) + $\nu$ CO (21) + $\nu$ CC (14) + $\delta$ COC (14)
28	1405		1427	1403	132.9	4.4	0.05	1424, 1428	1400, 1404	$\delta$ OH (32) + $\nu$ CN (26) + $\nu$ CC (21) + $\delta$ CCH (21)
29	1449		1472	1447	12.6	8.0	0.09	1472, 1484	1447, 1459	$\delta$ CH (48) + $\delta$ CC (21) + $\nu$ CN (13)
30	1565		1585	1558	29.4	17.7	0.16	1586, 1595	1559, 1568	$\nu$ CC (56) + $\delta$ CH (15) + $\delta$ CN (14)
31	1577	1580	1618	1590	107.2	43.9	0.37	1616, 1618	1589, 1590	$\nu$ CC (50) + $\nu$ CN (22) + $\delta$ CH (15)
32	1718	1714	1782	1707	45.4	53.4	0.35	1745, 1784	1672, 1709	$\nu$ C=O (90)
33	3058	3057	3165	3032	11.5	118.5	0.11	3163, 3180	3030, 3046	$\nu$ CH (100)
34	3092	3090	3193	3059	2.7	78.2	0.07	3191, 3197	3057, 3063	$\nu$ CH (100)
35	3161		3206	3071	5.0	199.5	0.18	3204, 3210	3069, 3075	$\nu$ CH (100)
36			3755	3597	99.8	143.9	0.07	3161, 3754	3028, 3596	$\nu$ OH (100)

$\nu$ ; stretching,  $\delta$ ; in plane bending,  $\gamma$ ; out of plane bending,  $\omega$ ; wagging,  $\tau$ ; torsion.  
 $I_{\text{IR}}$ ; IR intensities;  $S_{\text{Ra}}$ ; Raman scattering activities;  $I_{\text{Ra}}$ ; Raman intensities.

**Table 2.** The observed FT-IR, FT-Raman and calculated wavenumbers (in  $\text{cm}^{-1}$ ) using B3LYP/6-311++G(d,p) along with their relative intensities, probable assignments and total energy distribution (TED) of monomer and dimer conformers of 6-BrNA

Experimental		Monomer conformer (B3LYP)					Dimer conformer (B3LYP)		TED ( $\geq 10\%$ )
FT-IR	FT-Ra	Unscaled wavenumbers	Scaled wavenumbers	$I_{\text{IR}}$	$S_{\text{Ra}}$	$I_{\text{Ra}}$	Unscaled wavenumbers	Scaled wavenumbers	
1		66	65	3.2	0.2	0.01	61, 76	60, 75	$\tau$ CCCO (98)
2	83	71	70	0.0	0.0	0.00	38, 77	37, 76	$\omega$ 6-BrNA (94)
3	123	153	150	1.4	0.4	0.00	200, 202	197, 199	$\delta$ C-COOH (62) + $\delta$ CBr (31)
4		243	239	0.0	0.8	0.01	251, 259	247, 255	$\omega$ 6-BrNA (98)
5		246	242	2.1	5.2	0.03	247, 278	243, 273	$\nu$ CBr (46) + $\nu$ C-COOH (16) + $\delta$ CCN (12)
6	276	288	283	1.3	0.2	0.00	304, 324	299, 318	$\delta$ CBr (55) + $\delta$ CCC (33)
7	404	415	408	6.1	0.2	0.00	412, 413	405, 406	$\gamma$ CCCN (38) + $\gamma$ CCCC (22) + $\gamma$ CCCH (20)
8		454	446	41.2	0.1	0.00	465, 481	457, 473	$\nu$ CBr (28) + $\delta$ OCO (25) + $\nu$ C-COOH (21)
9	464	471	463	20.7	0.4	0.00	479, 481	471, 473	$\gamma$ CCCN (33) + $\gamma$ CCCH (21) + $\gamma$ CCCO (13) + $\gamma$ CCCC (13)
10	474	505	496	8.3	0.8	0.00	519, 547	510, 538	$\nu$ C-COOH (51) + $\delta$ CCC (20)
11	542	578	568	79.2	2.9	0.01	884	869	$\gamma$ OH (86)
12		636	625	3.2	6.4	0.45	637, 637	626, 626	$\delta$ ring def (85)
13	630	631	674	663	20.7	0.5	708, 724	696, 712	$\delta$ OCO (48) + $\delta$ CCC (13) + $\nu$ CBr (10)
14	712	730	718	9.7	0.0	0.00	723, 725	711, 713	$\gamma$ CCNC (52) + $\delta$ C-COOH (22) + $\gamma$ CCCC (11)
15	767	781	768	56.3	0.1	0.01	777, 780	764, 767	$\gamma$ CCCO (36) + $\gamma$ CCCH (30) + $\gamma$ OCOH (19)
16	812	809	804	790	46.5	24.5	821, 829	807, 815	$\nu$ CC (22) + $\delta$ CNC (18) + $\delta$ CCC (15) + $\nu$ C-COOH (15)
17	823	861	846	9.1	0.4	0.01	861, 861	846, 846	$\gamma$ CH (88)
18	848	966	950	2.3	0.7	0.02	969, 970	953, 954	$\gamma$ CH (93)
19	952	1007	990	0.3	0.1	0.00	1005, 1005	988, 988	$\gamma$ CH (90)
20	1015	1033	1015	16.8	2.0	0.04	1033, 1034	1015, 1016	$\delta$ CH (22) + $\delta$ CNC (21) + $\delta$ CCC (19) + $\nu$ CC (15)
21		1098	1079	112.6	32.6	0.62	1099, 1100	1080, 1081	Ring breathing (75)
22	1089	1092	1113	1094	290.2	3.3	1324, 1331	1301, 1308	$\nu$ CC (15) + $\nu$ CO (50) + $\delta$ CH (10)
23	1139	1142	1149	1129	4.0	4.0	1149, 1149	1129, 1129	$\delta$ CH (62) + $\nu$ CC (20)
24	1244	1207	1186	167.7	48.6	0.73	1160, 1163	1140, 1143	$\delta$ OH (48) + $\nu$ C-COOH (16)
25	1258	1296	1274	3.1	1.5	0.02	1287, 1289	1265, 1267	$\nu$ CC (49) + $\nu$ CN (42) + $\delta$ CH (10)
26	1281	1311	1289	3.7	4.6	0.06	1311, 1311	1289, 1289	$\delta$ CH (60) + $\nu$ CN (25)
27	1298	1306	1370	1347	147.8	23.6	1450, 1472	1425, 1447	$\delta$ OH (30) + $\nu$ CO (22) + $\nu$ CC(17) + $\delta$ COC (14)
28	1372	1392	1368	93.5	8.6	0.09	1391, 1392	1367, 1368	$\delta$ CH (38) + $\nu$ CC (23) + $\nu$ CN (20)
29	1419	1488	1463	58.3	8.2	0.07	1493, 1494	1468, 1469	$\delta$ CH (50) + $\nu$ CC (20) + $\nu$ CN (15)
30	1461	1589	1562	25.4	4.5	0.03	1587, 1588	1560, 1561	$\nu$ CC (64) + $\nu$ CN (15)
31	1579	1580	1620	1592	211.5	144.2	1589, 1620	1562, 1592	$\nu$ CC (51) + $\nu$ CN (18) + $\delta$ CH (18)
32	1678	1648	1791	1716	423.9	156.7	1689, 1736	1660, 1663	$\nu$ C=O (93)
33	3044	3044	3197	3063	1.8	73.5	3197, 3197	3063, 3063	$\nu$ CH (99)
34		3077	3197	3063	1.2	52.6	3199, 3199	3065, 3065	$\nu$ CH (100)
35	3088	3218	3083	3083	0.2	109.6	3218, 3218	3083, 3083	$\nu$ CH (100)
36		3769	3611	120.7	153.3	0.08	3112	2981	$\nu$ OH (100)

$\nu$ , stretching;  $\delta$ , in plane bending;  $\gamma$ , out of plane bending;  $\omega$ , wagging;  $\tau$ , torsion.  
 $I_{\text{IR}}$ , IR intensities;  $S_{\text{Ra}}$ , Raman scattering activities,  $I_{\text{Ra}}$ , Raman intensities.

coupled with other vibrations. However, the TED of C–N stretching is contributing 41 and 42% to the modes at 1272/1268  $\text{cm}^{-1}$  (IR/Ra) and 1258  $\text{cm}^{-1}$  (IR) for 2/6-Br-NA, respectively. These bands are predicted at 1264 and 1274  $\text{cm}^{-1}$  and in good agreement with the range given in the literature.

The ring stretching vibrations are very much important in the spectrum of pyridine and its derivatives, and are highly characteristic of the aromatic ring itself. The aromatic ring carbon–carbon stretching vibrations occur in the region 1430–1625  $\text{cm}^{-1}$ . In the present work, the C–C aromatic stretch is observed in the region 1449–1577  $\text{cm}^{-1}$  in the FT-IR spectrum, at 1580  $\text{cm}^{-1}$  in the FT-Raman spectrum (2-BrNA), 1419–1579  $\text{cm}^{-1}$  in the FT-IR spectrum and at 1580  $\text{cm}^{-1}$  in the FT-Raman spectrum (6-BrNA). These vibrations are in agreement with the theoretical assignment given by DFT. In our previous work, we have assigned the C–C vibrations at 1581  $\text{cm}^{-1}$  (IR) 1569  $\text{cm}^{-1}$  (Ra) for 2-chloronicotinic acid<sup>[7]</sup> and at 1582  $\text{cm}^{-1}$  (IR), 1584  $\text{cm}^{-1}$  (Ra) for 6-chloronicotinic acid.<sup>[8]</sup>

Mooney<sup>[27]</sup> assigned the vibrations of the C–X group (X = F, Cl, Br, and I) in the wavenumber range of 1129–480  $\text{cm}^{-1}$ . The heavier mass of bromine obviously makes the C–Br stretching mode to appear at longer wavelength region (200–480  $\text{cm}^{-1}$ ) as reported by Varsanyi.<sup>[28]</sup> The assignments of the C–Br stretching and deformation vibrations have been made on the basis of the calculated TED. The Raman band at 307  $\text{cm}^{-1}$  and the calculated value at 391  $\text{cm}^{-1}$  correspond to the C–Br stretching mode for 2-BrNA. The C–Br stretching modes are calculated at 242 and 446  $\text{cm}^{-1}$  for 6-BrNA. The C–Br in-plane bending vibrations are assigned to the Raman bands at 136, 232 and 123, 276  $\text{cm}^{-1}$  for 2-BrNA and 6-BrNA, respectively. The remainder of the observed and calculated wavenumbers and assignments are shown in Tables 1 and 2.

The infrared intensity for the title molecules from experimental fundamentals ( $\nu_{31}$ ) at 1577 and 1678  $\text{cm}^{-1}$  (for 2/6-BrNA) is very high, but the theoretical intensity of these fundamentals is not in the same order. This may be attributed to the inadequacy of the DFT methods as the basis set in predicting the intensities of the  $A'$  wavenumbers of the molecules. While the experimental intensity is very high for this mode, the calculated intensity is 107.2 and 211.5  $\text{km mol}^{-1}$  for the 2/6-BrNA C1 conformer. This mode corresponds to the C–C stretching. The largest value of the calculated intensity is 132.9  $\text{km mol}^{-1}$ , which corresponds to the  $\delta\text{OH}$  in-plane bending mode for 2-BrNA and 423.9  $\text{km mol}^{-1}$ , which corresponds to C=O stretching mode for 6-BrNA.

In general, our experimental infrared and Raman intensities are very high when compared with theoretical intensities at the lower wavenumber region. Among the calculated fundamentals, the best agreement between the experimental and calculated intensities is in the high wavenumber region (ca 3000–3200  $\text{cm}^{-1}$ ). While experimental and calculated high intensities may lead to the true identification in the assignments of fundamentals, low intensities may lead to the wrong identification in the assignment of fundamentals.<sup>[29]</sup> For such reasons, i.e. anharmonic effect, the vibrational intensity could not be estimated very accurately using quantum chemistry software.

The calculated wavenumbers for the dimer 2/6-BrNA are tabulated in Tables 1 and 2. As seen in the tables, the hydrogen-bonding effect through the carboxyl groups is clearly observed. This is in agreement with Karabacak and Kurt,<sup>[8]</sup> and Akkaya and Akyüz.<sup>[30]</sup>

## Conclusion

The FT-IR and FT-Raman spectra were recorded and the detailed vibrational assignment was presented for 2-bromonicotinic acid and 6-bromonicotinic acid, for the first time. The most stable monomer conformers of compounds were determined, and according to these results the dimer conformations were analyzed with DFT B3LYP/6-311++G(d,p) level of theory. The pyridine N atom-carboxylic acid OH group and the hydrogen bonding between a hydroxyl group O=COH were determined as dimer structure of 2- and 6-bromonicotinic acid. For both compounds, the vibrational wavenumbers were compared with experimental results. The difference between the corresponding wavenumbers (observed and calculated) is very small for most of fundamentals. Therefore, the results presented in this work for 2/6-BrNA indicates that this level of theory is reliable for prediction of both infrared and Raman spectra of the title compounds.

## Acknowledgements

This work was supported by the Scientific Research fund of Afyon Kocatepe University, Project No. 051.FENED.07. We thank Dr. Tahir Güllüođlu of Ahi Evran University, Kir\_ehir, Turkey, for the SQM program.

## Supporting information

Supporting information may be found in the online version of this article.

## References

- [1] S. Gao, J.-W. Liu, L.-H. Huo, Z.-Z. Sun, J.-S. Gao, S. W. Ng, *Acta Cryst.* **2004**, C60, m363.
- [2] W. B. Wright, G. S. D. King, *Acta Cryst.* **1953**, 6, 305.
- [3] A. Kutoglu, C. Scherlinger, *Acta Cryst.* **1983**, C39, 232.
- [4] N. K. Singh, D. K. Singh, *Synth. React. Inorg. Met.-Org. Chem.* **2002**, 32(2), 203.
- [5] P. Koczon, J. Cz. Dobrowolski, W. Lewandowski, A. P. Mazurek, *J. Mol. Struct.* **2003**, 655, 89.
- [6] O. Sala, N. S. Gonççalves, L. K. Noda, *J. Mol. Struct.* **2001**, 565(566), 411.
- [7] M. Karabacak, M. Cinar, M. Kurt, *J. Mol. Struct.* **2008**, 885, 28.
- [8] M. Karabacak, M. Kurt, *Spectrochim. Acta A* **2008**, 71, 876.
- [9] J. Baker, A. A. Jarzecki, P. Pulay, *J. Phys. Chem. A* **1998**, 102, 1412.
- [10] M. V. N. de Souza, S. M. S. V. Wardell, R. A. Howie, *Acta Cryst. E* **2005**, 61, o1347.
- [11] S. Long, M. Siegler, T. Li, *Acta Cryst. E* **2007**, 63, o279.
- [12] C. Lee, W. Yang, R. G. Parr, *Phys. Rev. B* **1988**, 37, 785.
- [13] A. D. Becke, *J. Chem. Phys.* **1993**, 98, 5648.
- [14] G. Rauhut, P. Pulay, *J. Phys. Chem.* **1995**, 99, 3093.
- [15] J. Baker, A. A. Jarzecki, P. Pulay, *J. Phys. Chem.* **1998**, A102, 1412.
- [16] M. J. Frisch, G. W. Trucks, H. B. Schlegel, G. E. Scuseria, M. A. Robb, J. R. Cheeseman, V. G. Zakrzewski, J. A. Montgomery, Jr., R. E. Stratmann, J. C. Burant, S. Dapprich, J. M. Millam, A. D. Daniels, K. N. Kudin, M. C. Strain, O. Farkas, J. Tomasi, V. Barone, M. Cossi, R. Cammi, B. Mennucci, C. Pomelli, C. Adamo, S. Clifford, J. Ochterski, G. A. Petersson, P. Y. Ayala, Q. Cui, K. Morokuma, D. K. Malick, A. D. Rabuck, K. Raghavachari, J. B. Foresman, J. Cioslowski, J. V. Ortiz, A. G. Baboul, B. B. Stefanov, G. Liu, A. Liashenko, P. Piskorz, I. Komaromi, R. Gomperts, R. L. Martin, D. J. Fox, T. Keith, M. A. Al-Laham, C. Y. Peng, A. Nanayakkara, M. Challacombe, P. M. W. Gill, B. Johnson, W. Chen, M. W. Wong, J. L. Andres, C. Gonzalez, M. Head-Gordon, E. S. Replogle, J. A. Pople, *GAUSSIAN 03, Revision A.9*, Gaussian, Inc., Pittsburgh, PA, **2003**.
- [17] B. G. Johnson, P. M. Gill, J. A. Pople, *J. Chem. Phys.* **1993**, 98, 5612.
- [18] A. E. Ozel, S. Kecel, S. Akyüz, *Vib. Spectrosc.* **2006**, 42, 325.
- [19] N. Sundaraganesan, S. Ilakiamani, H. Saleem, P. M. Wojciechowski, D. Michalska, *Spectrochim. Acta A* **2005**, 61, 2995.



- [20] G. Keresztury, S. Holly, J. Varga, G. Besenyi, A. Y. Wang, J. R. Durig, *Spectrochim. Acta A* **1993**, 49A, 2007.
- [21] G. Keresztury, J. M. Chalmers, P. R. Griffith (Eds.), *Raman Spectroscopy: Theory, Hand book of Vibrational Spectroscopy*, vol. 1, John Wiley & Sons Ltd.: New York, **2002**.
- [22] D. Lin-Vein, N. B. Colthup, W. G. Fateley, J. G. Grasselli, *The Handbook of Infrared and Raman Characteristic Frequencies of Organic Molecules*, Academic Press: San Diego, **1991**.
- [23] M. Silverstein, G. Clayton Basseler, C. Morill, *Spectrometric Identification of Organic Compounds*, Wiley: New York, **1981**.
- [24] N. Sundaraganesan, S. Ilakiamani, B. D. Joshua, *Spectrochim. Acta A* **2007**, 67, 287.
- [25] M. Kurt, *J. Raman Spect.* **2009**, 40, 67.
- [26] N. Sundaraganesan, C. Meganathan, B. Ananda, B. Dominic Joshua, C. Lapouge, *Spectrochim. Acta A* **2007**, 67, 830.
- [27] E. F. Mooney, *Spectrochim. Acta* **1964**, 20, 1021.
- [28] G. Varsanyi, *Assignments of Vibrational Spectra of 700 Benzene Derivatives*, Wiley: New York, **1974**.
- [29] J. E. del Bene, *J. Am. Chem. Soc.* **1979**, 101, 6184.
- [30] Y. Akkaya, S. Akyüz, *Vib. Spectrosc.* **2006**, 42, 292.